Available online at www.sciencedirect.com
SCIENCE DIRECT®
Journal of Crystal Growth 252 (2003) 382–390
JOURNAL OF CRYSTAL GROWTH
www.elsevier.com/locate/jcrysgro

Growth of $BaFe_{12}O_{19}$ thin films formed by reactive diffusion

V. Pankov[a,b,c], Å. Bartholdson[d], O. Stukalov[a], S. Smolenchuk[c], O. Babushkin[e,*], V. Gremenok[a]

[a] *Institute of Solid State Physics, Academy of Science Belarus, P. Brovki Str. 17, 220072 Minsk, Belarus*
[b] *Institute of General and Inorganic Chemistry, Academy of Science Belarus, Surganova Str. 9, 220072 Minsk, Belarus*
[c] *University of Technology of Belarus, Sverdlova Str.13, Minsk, Belarus*
[d] *Division of Physics, Luleå University of Technology, SE-971 87 Luleå, Sweden*
[e] *Division of Engineering Materials, Luleå University of Technology, SE-971 87 Luleå, Sweden*

Received 15 June 2002; received in revised form 30 November 2002
Communicated by D.T.J. Hurle

Abstract

Thin films of $BaFe_{12}O_{19}$ have been grown on (00 *l*) oriented α-Fe_2O_3 single crystal substrates. The initial stages of the reaction between $BaFe_2O_4$ thin films and hematite single crystals have been investigated using AFM and SEM. The microstructure studies showed that (00 *l*) oriented $BaFe_{12}O_{19}$ microcrystallites formed during annealing at 900–1100°C. It was concluded that the surface diffusion had a dominating role in formation of thin $BaFe_{12}O_{19}$ films. Crystal growth was performed by stacking of layers with the thickness 2.3 nm, correlated with the *c*-parameter of the $BaFe_{12}O_{19}$ unit cell.

PACS: 68.35−p; 68.35.Bs; 66.30.−h; 64.70.kb

Keywords: A1. Crystal morphology; A1. Diffusion; A1. Growth models; A1. Interfaces; A1. Nucleation; B1. Ferrites.

1. Introduction

M-type hexagonal ferrites ($BaFe_{12}O_{19}$ and $SrFe_{12}O_{19}$) are known for their high magnetocrystalline anisotropy and their chemical stability [1]. They have been used in bulk form for many applications thanks to their hard magnetic properties, for example, as permanent magnets. Recently, ferrites have drawn a substantial interest as materials showing good recording characteristics for both longitudinal and vertical recording [2–4].

The hexagonal ferrite films have been deposited by a number of techniques, such as conventional DC and RF sputtering, facing target sputtering and pulsed laser deposition, using in situ annealing [4–14]. At the same time high-temperature treatment in vacuum is a costly process accompanied with the necessity to use complicated equipment [15]. Here the method of reactive diffusion for making $BaFe_{12}O_{19}$ film is proposed [16]. Then the $BaFe_{12}O_{19}$ film is formed due to reaction between the $BaFe_2O_4$ film deposited by laser ablation and the substrate surface presented by α-Fe_2O_3 single crystal cut along the [00 *l*] plane. This reaction can

*Corresponding author.

0022-0248/03/$ - see front matter
doi:10.1016/S0022-0248(02)02460-0

be written as

$$BaFe_2O_4 + 5Fe_2O_3 = BaFe_{12}O_{19}.$$

As a result a very thin film is formed. This film can be a subject for investigations of the earlier stages of solid-state reactions.

It should be noted that during sintering of a thin film by conventional techniques, properties of the film degrade due to interaction with the substrate and as a consequence of the formation of undesired intermediate phases. Reactions at the film–substrate boundary have been reported in a number of investigations devoted to thin film deposition through electronic spraying, molecular beam epitaxy and laser ablation. Obviously, the change of the chemical composition will lead to degradation of the functional properties of the films. An important task is to avoid formation of undesirable phases when thin films based on multicomponent oxide systems are sintered.

The suggested method of making thin films by reactive diffusion during interaction between deposited precursor film with substrate eliminates the formation of intermediate layers on film–substrate boundaries. It implies correct selection of proper components participating in the process of reactive diffusion. The selection of the reactive couples can be made on the basis of detailed examination of existing phase diagrams of the systems.

Several investigations of solid-state reactions in the formation of thin films based on spinel structure are mentioned in Refs. [15–17]. Similar investigations on the formation of $BaFe_{12}O_{19}$ films by reactive diffusion have not been made so far, in spite of their growing practical application.

2. Experimental procedures

Thin films of $BaFe_{12}O_{19}$ were formed on single-crystals of α-Fe_2O_3 substrates cut along the basal (00*l*) plane. Hematite single crystals were made from a melt of iron oxide and β-$NaFeO_2$ [18]. The concentration of Fe_2O_3 in the melt was chosen to be 30 wt%. Hematite crystallization was performed in the temperature interval 975–1090°C. The substrate was rectangular, with a $5 \times 5\,mm^2$ face exposed to film deposition. Prior to film deposition the substrate was cleaned with organic solvents. Then the film was deposited on the substrate by pulsed laser deposition without preheating of the substrate.

A pulsed KrF excimer laser, operated at 1 Hz with wavelength $\lambda = 1.06\,\mu m$, was line-focused on a rotating polycrystalline $BaFe_2O_4$ target. The laser beam passed into a vacuum chamber, and then it was focused on the surface of the rotating target by a lens with a focal length of 500 mm. The distance between target and substrate was 6 cm. The angle of incidence of the laser beam to the target was 45°. The pulse time was 1×10^{-3} second. The thickness of the formed film was directly related to the energy and total number of pulses.

The deposited $BaFe_2O_4$ films were annealed at 900°C, 1000°C and 1100°C for 1 h in order to initiate the solid-state reaction with formation of a $BaFe_{12}O_{19}$ thin film. The thickness of the formed film was within the interval 50–280 nm, depending on the temperature.

The phase composition of the films was characterized by DRON (Russian) and Philips X-Pert multipurpose research diffractometer (MRD) systems. The microstructures of the formed films were investigated with a Hitachi S-806 scanning electron microscope and two different atomic force microscopes (AFM), Fentoskan-001 and digital instruments Nanoscope II. The images were recorded using contact mode, with both constant-height and constant-force modes. Silicon-nitride tips were used on cantilevers with nominal spring constants of 0.8 and $0.58\,N\,m^{-1}$ as specified by the manufacturer. The samples were washed in ethanol before imaging if needed.

3. Results

Examination by X-ray diffraction (XRD) of the precursor film of $BaFe_2O_4$ deposited by laser deposition on α-Fe_2O_3 substrates, showed its amorphous state (Fig. 1a). All diffraction patterns of crystallized films showed only the Bragg reflections corresponding to the $BaFe_{12}O_{19}$ crystal planes (0 0 6) with *d*-space 3.795 Å, (0 0 8) with

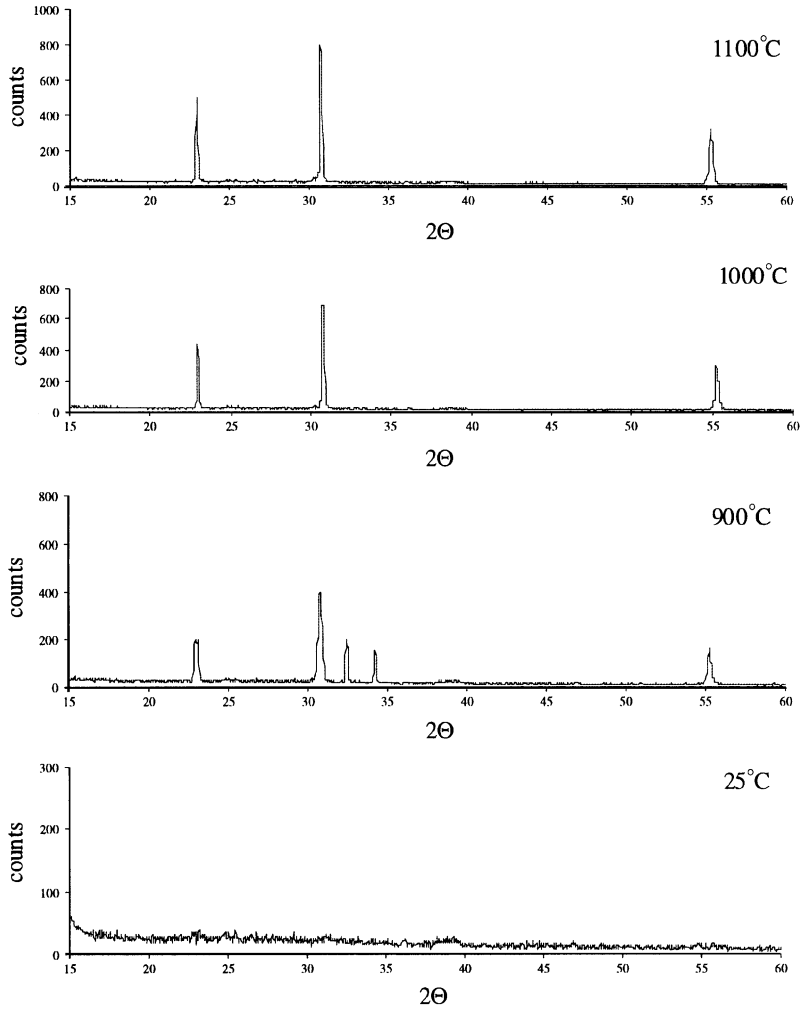

Fig. 1. X-ray powder diffraction patterns of: (a) the amorphous $BaFe_2O_4$ precursor film on the α-Fe_2O_3 substrate, and (b–d) crystallized $BaFe_{12}O_{19}$ films formed after treatment at, respectively, 900°C, 1000°C and 1100°C.

$d = 2.882$ Å and (0 0 14) with $d = 1.657$ Å. The diffraction patterns of films annealed at 1000°C and 1100°C did not show the highest intensity peaks from the planes (1 1 0), (1 0 7), (1 1 4) or (2 0 3). The absence of these peaks strongly indicates that these films were grown with the (00 *l*) preferred orientation (Fig. 1c,d). At the same time, for the film annealed at 900°C, some differences in diffraction patterns were noticed. A number of additional peaks relating to the planes (1 1 4) and (1 0 7) were observed (Fig. 1b). This fact can be due to a lower degree of texturing caused by formation of more randomly oriented crystals with smaller sizes. Nevertheless, the powder diffraction results demonstrate that, in the initial stages of the film growth, a single crystal of $BaFe_{12}O_{19}$ phase is formed on the α-Fe_2O_3 substrate predominantly parallel to the (00 *l*)-crystal plane (also during further growth).

The dimensions and shapes of the grains of the $BaFe_{12}O_{19}$ phase were examined by electron microscopy. It was determined that, for film annealed at 900°C, the grain sizes were in the range 0.2–0.3 μm (Fig. 2a). The increase of annealing temperature up to 1100°C leads to a pronounced increase of grain dimensions up to

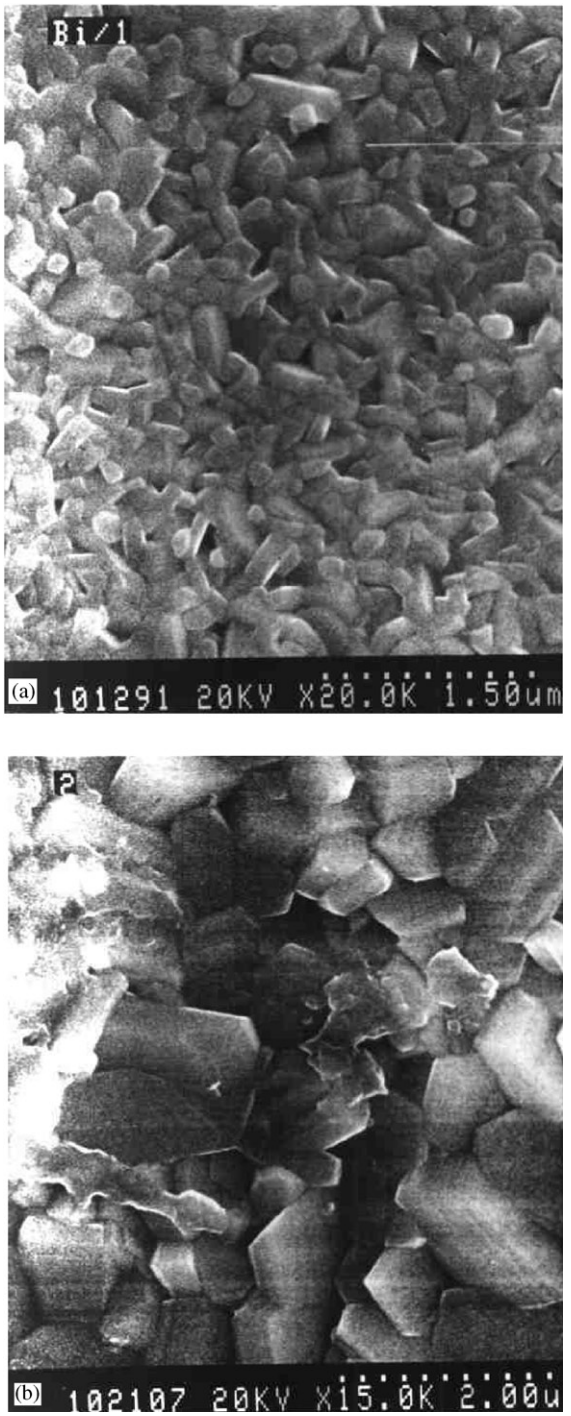

Fig. 2. SEM images of the $BaFe_{12}O_{19}$ films formed on α-Fe_2O_3 substrate at: (a) 900°C and (b) 1100°C.

1–1.5 μm (Fig. 2b). At this temperature the shape of the grains becomes hexagonal with sharp edges (Fig. 2b). Grains formed at 900°C, however, showed more random orientation relative to the substrate plane (Fig. 2a).

Special attention was paid to atomic force microscopy (AFM) investigations, which gave

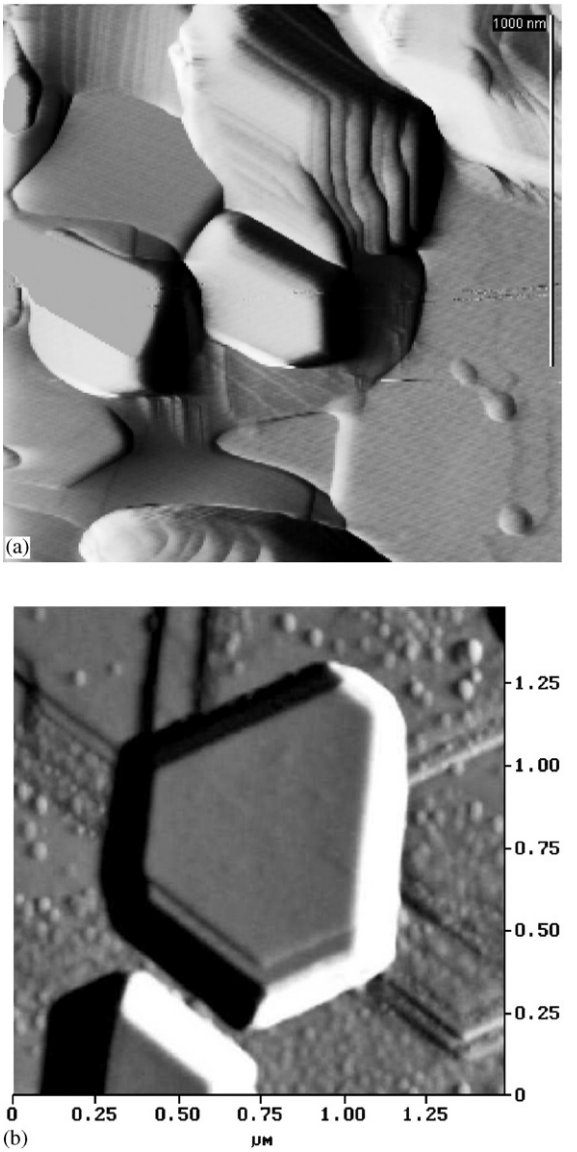

Fig. 3. AFM images of the $BaFe_{12}O_{19}$ films formed on the α-Fe_2O_3 surface at: (a) 1000°C and (b) 1100°C, showing the different sizes of the crystallites.

opportunity to evaluate the character of surface and film profile characteristics of formed grains and detection of inclusions and growing faces of a crystal. Examination of crystallized films of $BaFe_{12}O_{19}$ showed a typical hexagonal structure of grains and demonstrated different stages of crystal growth (Fig. 3a,b). It was established that the thickness of some dislocations was in the range of 2–3 nm (Fig. 4a,b), which is equal to the *c*-dimension of the $BaFe_{12}O_{19}$ unit cell, estimated as 2.32 nm [19,20].

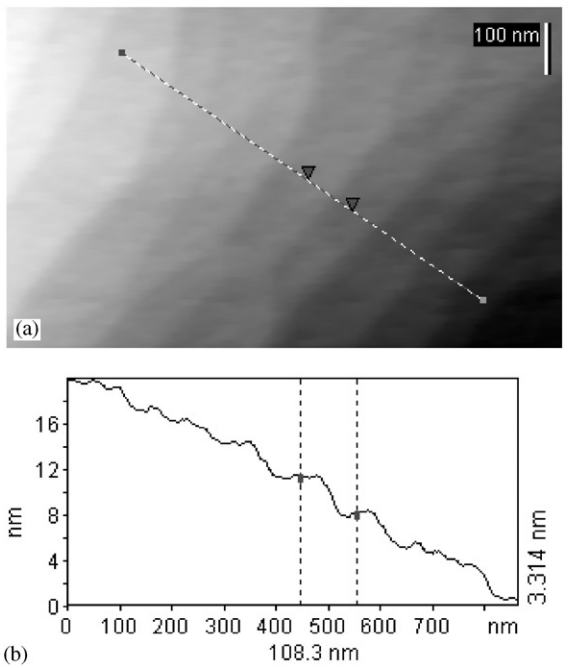

Fig. 4. AFM study of the edge of a $BaFe_{12}O_{19}$ crystallite, situated at the surface of a 130 nm thick film formed after sintering at 900°C: (a) Visible steps at the edge of the crystallite; (b) Profile of the edge, along the line in (a), with steps approximately 3 nm high.

In order to study the details of the first stages of crystal formation, we prepared some samples with a deposited precursor $BaFe_2O_4$ in the form of discrete small drops on the Fe_2O_3 substrate. Such small crystallized spheres (Fig. 5a) were formed after annealing of the $BaFe_{12}O_{19}$ film. Examination of this type of sample clearly showed how deepened profiles in the Fe_2O_3 substrate were formed around single crystals of $BaFe_{12}O_{19}$. They were similar to profiles of newly formed $BaFe_{12}O_{19}$ crystals (Fig. 5b). AFM images showed that a new phase crystallized due to growth of a number of new planes on the surface (Fig. 6) and we conclude that in this process the surface diffusion obviously played a substantial role.

In Fig. 7 one can clearly see the new crystallized phase in the shape of plate-like 3D islands. The structure is hexagonal and in some places the crystallites have almost perfect triangular shape. The corresponding edges of the islands are parallel to each other (Fig. 8a), showing preferred directions due to the orientation of the substrate

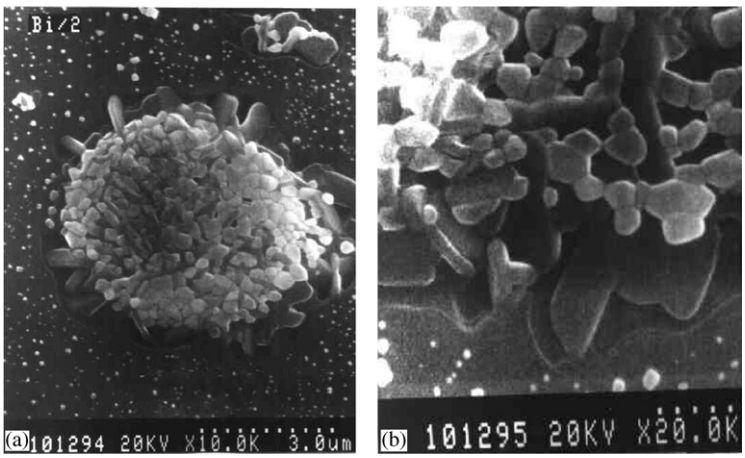

Fig. 5. SEM images of: (a) a $BaFe_{12}O_{19}$ sphere formed on the α-Fe_2O_3 substrate at 900°C and (b) a fragment of the interface boundary between the sphere ($BaFe_{12}O_{19}$) and the substrate (α-Fe_2O_3).

surface. No steps have been observed on top of these crystallites, indicating that the growth process has stopped. An additional type of outgrowth can be seen between the islands (Fig. 8a), i.e. smaller spherical grains (20–70 nm in diameter). This type has been reported earlier [24]. Moreover, these small spherical grains are often located along step edges, roughly 1–5 nm high. The step edges follow the same preferred directions as the edges of the islands.

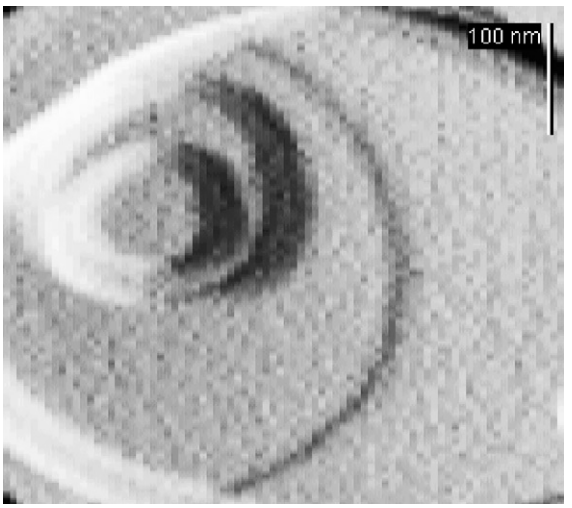

Fig. 6. AFM image of a spiral growing $BaFe_{12}O_{19}$ crystallite.

4. Discussion

We selected $BaFe_2O_4$ as a precursor for deposition on an α-Fe_2O_3 substrate for further sintering into the formation of $BaFe_{12}O_{19}$ film, because according to the BaO–Fe_2O_3 phase diagram, only one $BaFe_{12}O_{19}$ phase [20] is formed according to the reaction

$$BaFe_2O_4 + 5Fe_2O_3 = BaFe_{12}O_{19}.$$

This statement was tested by calcination of diffusion couples consisting of preliminary calcined plates of $BaFe_2O_4$ and Fe_2O_3 in the temperature range 900–1100°C. Examination by electron microprobe of the reactive zone between these diffusion couples showed only one Ba $Fe_{12}O_{19}$ phase as a reaction product. It was established that this phase crystallized basically on the Fe_2O_3 substrate, which indicated diffusion of barium ions and oxygen transport into the Fe_2O_3 surface. This type of solid-state reactions can be found for instance in powdered oxides. The mechanism of the formation of $BaFe_{12}O_{19}$ in the $BaFe_2O_4$–Fe_2O_3 system can then analogously be explained by transport of barium and oxygen ions into the grain boundary of $BaFe_2O_4$/ Fe_2O_3, with crystallization of $BaFe_{12}O_{19}$ as the reaction product.

However, it must be emphasized that a thermodynamically powdered macroscale system in the frame of which the mechanism of the reaction formation of $BaFe_{12}O_{19}$ was considered, may not

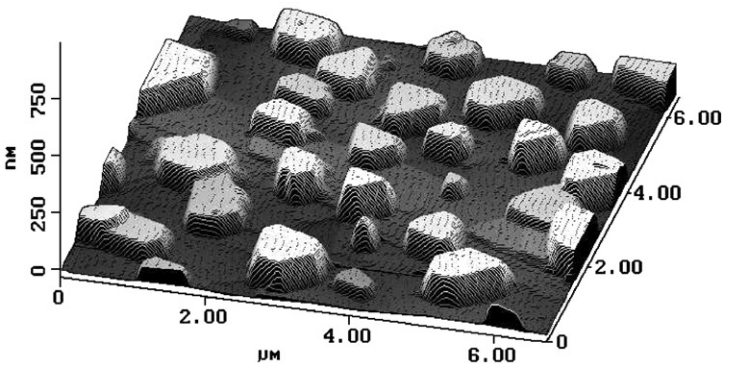

Fig. 7. AFM image showing fully grown hexagonal $BaFe_{12}O_{19}$ crystallites. The height-scale is deliberately exaggerated. The crystallites should still be considered as thin plates.

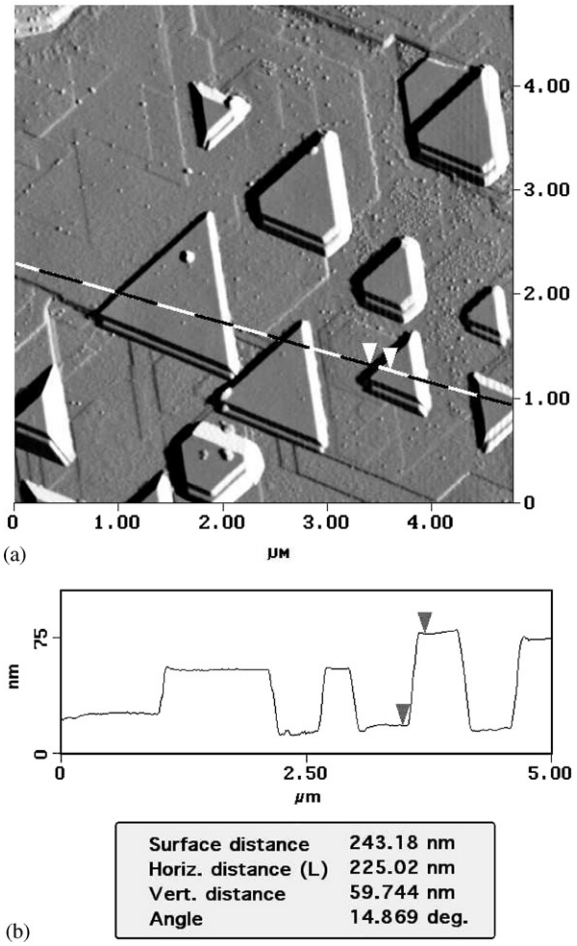

Fig. 8. (a) Triangular crystallites with corresponding edges parallel to each other, influenced by the orientation of the substrate surface. In the upper left part of the image small spherical grains are located between the 3D islands mainly at step edges. (b) Profile along the line in (a).

always be valid for nanoscale thin film systems. Here it was established that surface diffusion is more important than the volume diffusion for the thin film. As mentioned earlier, the thicknessess of stacking layers were 2-3 nm (Fig. 4), which is consistent with the *c*-dimension of the $BaFe_{12}O_{19}$ unit cell, estimated to be 2.32 nm [19,20]. It seems that in this case the rate-controlling step of crystal growth will be the kinetic of interfacial reaction rather than a diffusion of components through the layer of the formed product. A similar phenomenon was observed for NiO/Al_2O_3 heterostructures, in which the film of $NiAl_2O_4$ was formed [21]. The thickness of this film increased linearly with time, and not according to the parabolic law for diffusion-controlled processes.

A possible mechanism of the $BaFe_{12}O_{19}$ phase formation at the $BaFe_2O_4$/ Fe_2O_3 heterostructure is proposed (Fig. 9a–d) based on the data of crystal morphology at different stages of the growth. In fact, a newly formed nucleus of the $BaFe_{12}O_{19}$ phase grows along the substrate surface more quickly than in the direction perpendicular to the α-Fe_2O_3 substrate surface because of a lower activation energy of the surface diffusion. Due to the fact that the rate of $BaFe_{12}O_{19}$ growth in a basal plane (*a*–direction) exceeds the velocity of growth in the c–direction [22], the nucleus of $BaFe_{12}O_{19}$ gradually transformed into thin plates located parallel to the substrate surface (Fig. 9b).

As mentioned earlier, the ions diffuse to the growing face of a crystal. At the same time the nearby sites of α-Fe_2O_3–$BaFe_2O_4$ are gradually consumed, resulting in deepening around the formed $BaFe_{12}O_{19}$ crystals (Fig. 9b). It was

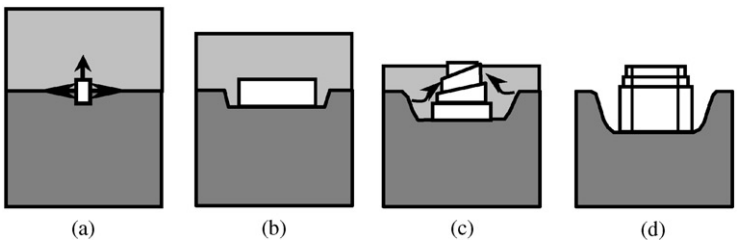

Fig. 9. Schematic presentation of different stages of the $BaFe_{12}O_{19}$ crystal growth: (a) Formation of a nucleus of the $BaFe_{12}O_{19}$ phase; (b) The nucleus grows faster along the α-Fe_2O_3 substrate surface than in the perpendicular direction, leading to a transformation to a thin plate parallel to the substrate surface; (c) Upper layers appear as a result of spiral growth of the first layer caused by surface diffusion; (d) Further crystallization leads to perfection of the grain shape, i.e., hexagonal and triangular plates with sharp edges.

observed that, above a certain critical size of a crystal in the *a*-direction, a second layer appeared, which was formed in the *c*-direction of the hexagonal $BaFe_{12}O_{19}$ structure. It was noticed that the upper layer did not appear from nuclei formed on the (00 *l*) plane of the first layer, but it was a result of spiral growth of the first layer caused by surface diffusion (Fig. 9c). AFM studies showed spiral-type pyramids formed during growth of the $BaFe_{12}O_{19}$ film (Fig. 6). Further crystallization led to perfection of the grain shape and transition of grain shape from a rounded type to the shape of hexagonal plates with sharp edges (Fig. 9d). It should be noted that even for hexagonal grains the stacked layers were still visible (Fig. 3b). This indicates the dominating role of surface diffusion during formation and growth of $BaFe_{12}O_{19}$ crystals.

It is known that topotactic reactions lead to formation of phases that are crystallographically oriented with correlation to the orientation of the crystallite substrate. Our structural analysis data, including XRD, electron microscopy and AFM, demonstrate that the orientation relationship between $BaFe_{12}O_{19}$ and α-Fe_2O_3 is $[0001]_{BaFe_{12}O_{19}} \parallel [0001]_{\alpha Fe_2O_3}$. The crystallization and growth of Ba–hexaferrite on the basal α-Fe_2O_3 surface were directly influenced by the crystallography of α-Fe_2O_3 surfaces. It means that as a consequence of different crystallographic parameters of α-Fe_2O_3 and $BaFe_{12}O_{19}$ there exists a lattice misfit classically accommodated by a hexagonal array of misfit edge dislocations at the interface. In addition, as shown in Ref. [23], the relationship at the interface involves special rotations between crystals, for instance in the case of growth of $CaAl_{12}O_{19}$ on an α-Al_2O_3 substrate, which establishes a definite coincident–site lattice disorientation.

5. Conclusions

In this study thin amorphous films of $BaFe_2O_4$ were deposited on (00 *l*)-oriented α-Fe_2O_3 substrates using a pulsed-laser deposition technique. The resulting diffusion couples were then reacted at high temperatures in air to initiate the reaction between the thin film and bulk substrate to form the $BaFe_{12}O_{19}$ layers.

X-ray examination of the films crystallized at 900–1100°C demonstrated that, in all cases, the $BaFe_{12}O_{19}$ phase was formed as a product of reaction between the precursor $BaFe_2O_4$ deposited on the substrate and the surface of the α-Fe_2O_3 substrate. The crystallographic relationship between α-Fe_2O_3 and $BaFe_{12}O_{19}$ was determined as $(0001)_{BaFe_{12}O_{19}} \parallel (0001)_{\alpha Fe_2O_3}$.

It was demonstrated that surface diffusion has the main role in crystallization of plate-like grains of $BaFe_{12}O_{19}$. The crystal faces were formed by layer stacking. It was established that the thickness of each layer was compatible with the value 2.3 nm for the *c*-dimension of the $BaFe_{12}O_{19}$ unit cell.

Application of the AFM technique revealed that a crystal of $BaFe_{12}O_{19}$ grows by stacking layer upon layer, forming a spiral. Further development of the crystallization process leads to perfection of the grain shape from rounded to hexagonal plates with sharp edges. The orientation of the edges was influenced by the crystallography of the substrate surface.

References

[1] D.E. Speliotis, IEEE Trans. Magn. 25 (1989) 4048.
[2] S. Yamamato, Y. Nakamura, S. Iwasaki, IEEE Trans. Magn. 23 (1987) 2070.
[3] S. Honda, K. Ouchi, S. Iwasaki, J. Appl. Phys. 75 (1994) 5484.
[4] M. Matsuoka, Y. Hoshi, M. Naoe, S. Yamanaka, IEEE Trans. Magn. 21 (1984) 800.
[5] A. Morisako, M. Matsumoto, M. Naoe, IEEE Trans. Magn. 24 (1988) 3024.
[6] N. Matsushita, K. Noma, M. Naoe, IEEE Trans. Magn. 30 (1994) 4053.
[7] K. Sin, M. Sivertsen, J.H. Judy, J. Appl. Phys. 75 (1994) 5972.
[8] A. Morisako, M. Matsumoto, M. Naoe, IEEE Trans. Magn. 22 (1986) 1146.
[9] J. Li, S.S. Rosenblum, W. Nojima, H. Hayashi, R. Sinclair, IEEE Trans. Magn. 31 (1995) 1749.
[10] D.E. Laughlin, B. Cheong, Y.C. Feng, D.N. Lambeth, Scr. Metall. Mater. 33 (1995) 1525.
[11] S.S. Rosenblum, H. Hayashi, R. Sinclair, IEEE Trans. Magn. 30 (1994) 4047.
[12] P. Papakonstantinou, R. Atkinson, I.W. Salter, R. Gerber, J. Magn. Soc. Japan S1 (1995) 177.
[13] R. Atkinson, I.W. Salter, J. Xu, Appl. Opt. 31 (1992) 4847.

[14] C.A. Carosella, D.B. Chrisey, P. Lubitz, J.S. Horwitz, J. Appl. Phys. 71 (1992) 5107.
[15] X. Sui, M.H. Kruder, Appl. Phys. Lett. 63 (1993) 1582.
[16] M.T. Johnson, C.B. Carter, Microsc. Microanal. 4 (1998) 141.
[17] D.E. Speliotis, J.P. Judge, W. Lynch, J. Burbage, IEEE Trans. Magn. 29 (1993) 3625.
[18] B.A. Murachev, A.B. Rosantsev, A.H. Sidorov, Publ. of the Moscow Technol Inst. 133 (1984) 21.
[19] J.D. Dunitz, L.E. Orgel, J. Phys. Chem. Solids. 3 (1957) 318.
[20] F. Haberey, IEEE Trans. Magn. 23 (1987) 29.
[21] P.G. Kotula, C.B. Carter, Phys. Rev. Lett. 77 (1996) 3367.
[22] P. Gornet, Prog. Crystal Growth Charact. 20 (1990) 263.
[23] M.P. Mallamaci, K.B. Sartain, C.B. Carter, Philos. Mag. A 77 (1998) 561.
[24] X.Y. Zhang, C.K. Ong, S.Y. Xu, H.C. Fang, Appl. Surf. Sci. 143 (1999) 323.